International Journal for Housing Science and Its Applications
Publish August 5, 2025. Volume 46, Issue 3 Pages 4376-4386

https://doi.org/10.70517/ijhsa463374

Research on remote control of power system based on adaptive control algorithm

Yu Yu[1], Yu Wang[1,*], Shucui Tan[2], Shining Chen[1] and Yuqian Mo[1]
[1] Nanning Power Supply Bureau of Guangxi Power Grid Co., Ltd., Nanning, Guangxi, 535000, China
[2] Yulin Power Supply Bureau of Guangxi Power Grid Co., Ltd., Yulin, Guangxi, 537000, China
Corresponding authors: (e-mail: Wangyu_1975@outlook.com).

Abstract For the problem of the existence of time delay in information transmission in power system which affects the stability of power system, this paper takes the remote control of the stability of power system as the research purpose. Radial Basis Function (RBF) neural network is introduced to define the adaptive control law for discrete nonlinear systems. Thus, a discrete adaptive neural network is constructed to estimate the unknown parameters and uncertainties within the power system. Then for the single machine infinity power system, establish a more realistic nonlinear generalized system mathematical model, for the analysis of this paper to provide a theoretical basis for research. For the optimization of power system stabilizer when the power system generates low-frequency oscillations, the Mothfly Flame (MFO) algorithm is selected for the coordinated optimization and tuning of controller parameters. Based on the multi-objective function, the optimal parameters of the controller are optimally solved under different time delays. Combining the above, the design of remote control strategy for power system based on adaptive control is completed. In the numerical simulation experiment, the coordinated power system controller starts to converge in about 1s, and the overall oscillation amplitude is small. The excellent robustness of the power system controller in remote control based on adaptive control algorithm is demonstrated.

Index Terms RBF neural network, stand-alone infinite power system, mothballing algorithm, adaptive control law

I. Introduction

As an indispensable infrastructure of modern society, the stable and efficient operation of the power system is vital to maintain social operation and ensure normal production and life [1]. With the increasing demand for electricity, the scale and complexity of power transmission and distribution projects are also increasing [2]. The traditional manual operation mode gradually appears to be difficult to cope with the enormous pressure of the power system and the rapidly changing operating environment, and the automated remote control technology of the power system comes into being [3], [4]. The automatic remote control of the power system is through the meticulous analysis of each link and part, and then the results are fed back to the operator, who can make corresponding adjustments according to the actual situation on the spot, thus ensuring the smooth progress of the work [5]. In order to improve the safety, reliability and operational efficiency of the power system, research is carried out around the application strategy of intelligent remote control technology in the power system [6], [7].

In today's rapidly developing electric power industry, intelligence has become an important trend in the development of electrical automation remote control systems. By integrating advanced artificial intelligence technology and big data analysis means, the intelligent system can realize more accurate and efficient operation and management, and improve the overall performance and safety of substations [8], [9]. The integration of intelligent algorithms improves the self-learning and self-adaptive ability of the power system operation, enabling it to make intelligent decisions based on real-time data and environmental changes, and realizing automated operation control [10]-[12]. This intelligent feature not only improves the response speed and accuracy of the system, but also can predict potential problems and take corresponding measures to effectively reduce operational risks [13], [14]. Intelligent systems are also able to optimize energy utilization, improve the energy efficiency and stability of the system, and provide strong support for the sustainable development of the power system [15].

This paper firstly analyzes the structural principle and approximation ability of radial basis function neural network, designs adaptive control law for discrete nonlinear system, and forms discrete adaptive neural network. Secondly, it elaborates the mathematical modeling process and steps of single-machine infinite excitation control system, and constructs the mathematical model. Again, the mothballing algorithm is introduced as the parameter optimization method of the power system controller. At the same time, the PID controller is chosen as the controller of the power system in this paper, and the optimal parameter solving steps based on the objective function are

explained. Within the framework of the power system mathematical model, the discrete adaptive neural network and the mothballing algorithm are integrated to propose the remote control strategy of the power system based on the adaptive control algorithm. Finally, application simulation and numerical simulation experiments of the power system are carried out to test the feasibility and reliability of the designed strategy. The effects of different parameters on the performance of the controller based on the proposed strategy are explored.

II. Remote control strategies for power systems

II. A.Discrete Adaptive Neural Networks

In the late 1980s, the radial basis function (RBF) technique was firstly invoked in neural network design, which led to the construction of RBF neural networks. As an efficient feed-forward network, this neural network not only has the best approximation performance, but also effectively solves the local minima problem. It is proved that the RBF function neural network has the ability to approximate continuous functions with arbitrary accuracy, making it an effective tool for analyzing the unknown laws of complex systems. It is a three-layer feed-forward network architecture, including the input layer, the hidden layer and the output layer of the neural network. The RBF neural network can be represented as a multi-input, single-output topology as shown in Fig. 1.

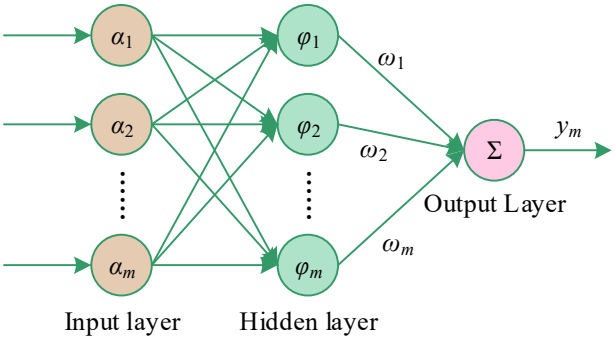

Figure 1: RBF neural network structure

The neural network is mapped from the input layer to the hidden layer in a nonlinear mapping fashion, using a Gaussian function as the basis function. The output of the j neuron in the hidden layer can be expressed as equation (1):

$$\varphi_j(\alpha) = \exp\left(-\frac{\|a - c_j\|^2}{2b_j^2}\right) \tag{1}$$

The output of the RBF neural network can be expressed as equation (2):

$$y_m = \sum_{i=1}^{m} w_{ij} \exp\left(-\frac{1}{2v^2}\|\alpha_p - c_i\|^2\right) \tag{2}$$

The new stabilizing adaptive control strategy, which distinguishes itself from the traditional method of adaptive law design that mainly relies on the estimation of network weights, employs the estimation error of the network weights to design the adaptive law and simplifies the design process of the control system by introducing auxiliary control signals. In the following, a controller based on adaptive RBF neural network is designed for discrete nonlinear systems.

Consider the following nonlinear discrete system as in equation (3):

$$y(K+1) = F[x(K)] + u(K) \tag{3}$$

where $y(K)$ is the discrete system output. $x(K) = [y(K), y(K-1), \cdots, y(K+1-n)]^T$ is the state vector of the system. $u(K)$ is the control input and the nonlinear smooth function $f: R^n \to R$ is assumed to be unknown.

Define the tracking error as in equation (4):

$$\varepsilon(K) = y(K) - y_d(K) \tag{4}$$

Since $F[x(K)]$ is unknown in the nonlinear discrete system, the powerful approximation property of the RBF neural network is applied to estimate the function $F[x(K)]$. Thus the output estimate of the neural network is equation (5):

$$\hat{F}[x(K)] = \hat{\omega}(K)^T \varphi[x(K)] \tag{5}$$

where $\hat{\omega}(K)$ is the neural network output weight vector and $\varphi[x(K)]$ is the Gaussian basis function.

For any given non-zero approximation error e_F, some ideal weight vector ω^* can always be found to satisfy equation (6):

$$F(x) = \hat{F}(x, \omega^*) - e(x) \tag{6}$$

where $e(x)$ represents the optimal error level that the neural network can achieve during the approximation process and $|e(x)| < e_F$.

Then the neural network approximation error is equation (7):

$$\begin{aligned} \tilde{F}[x(K)] &= F[x(K)] - \hat{F}[x(K)] \\ &= \hat{F}(x, \omega^*) - e[x(K)] - \hat{\omega}(K)^T \varphi[x(K)] \\ &= -\tilde{\omega}(K)^T \varphi[x(K)] - e[x(K)] \end{aligned} \tag{7}$$

where $\tilde{\omega}(K) = \hat{\omega}(K) - \omega^*$. The asymptotic error dynamic equation is equation (8):

$$\varepsilon(K+1) + g_a \varepsilon(K) = 0 \tag{8}$$

where $|g_a| < 1$, then $\varepsilon(K)$ tends to zero under any given initial condition.

After utilizing the approximation performance of the RBF neural network to deal with the system problem containing unknown parameters, the control law of the system can be designed as Eq. (9) based on Eq. (3):

$$u(K) = y_d(K+1) - \hat{F}[x(K)] - g_a \varepsilon(K) \quad (2-34) \tag{9}$$

Substituting equation (9) into equation (3) yields equation (10):

$$\varepsilon(K+1) = \tilde{F}[x(K)] - g_a \varepsilon(K) \tag{10}$$

Then we have equation (11):

$$\varepsilon(K) + g_a \varepsilon(K-1) = \tilde{F}[x(K-1)] \tag{11}$$

The above equation can also be expressed as equation (12):

$$\varepsilon(K) = T^{-1}(\tau^{-1}) \tilde{F}[x(K-1)] \tag{12}$$

where $T(\tau^{-1}) = 1 + g_a \tau^{-1}$. τ^{-1} is the discrete delay factor.

The design generalization error function is equation (13):

$$\varepsilon_a(K) = \mu \left[\varepsilon(K) - T^{-1}(\tau^{-1}) \nu(K) \right] \tag{13}$$

where $\mu > 0$ and $\nu(K)$ is the defined auxiliary signal.

Substituting the tracking error Eq. (12) into the generalization error Eq. (13) yields Eq. (14):

$$\begin{aligned} \varepsilon_a(K) &= \mu T^{-1}(\tau^{-1}) \left[\tilde{F}[x(K-1)] - \nu(K) \right] \\ &= \mu \frac{1}{1 + g_a \tau^{-1}} \left[\tilde{F}[x(K-1)] - \nu(K) \right] \end{aligned} \tag{14}$$

i.e., equation (15):

$$\varepsilon_a(K-1) = \frac{\mu[\tilde{F}[x(K-1)] - \nu(K)] - \varepsilon_a K}{g_a} \tag{15}$$

In order to ensure the stability of the system in the presence of non-zero approximation error e_F, the generalization error $\varepsilon_a(K)$ is chosen to define the following adaptive law, and the design of the adaptive control law is equation (16):

$$\Delta\hat{\omega}(K) = \begin{cases} \dfrac{\mu}{\delta h_a^2} \varphi[x(K-1)] \varepsilon_a(K), & |\varepsilon_a(K)| > \dfrac{e_F}{H} \\ 0, & |\varepsilon_a(K)| \le \dfrac{e_F}{H} \end{cases} \tag{16}$$

where $\Delta\hat{\omega}(K) = \hat{\omega}(K) - \hat{\omega}(K-1)$. The δ and H are strictly positive constants.

In the process of analyzing the stability of the system by applying Lyapunov's method, in order to ensure that the error $\varepsilon_a(K)$ gradually decreases and eventually approaches zero, it is necessary to introduce an auxiliary control signal $\nu(K)$, which can further ensure that the tracking error $\varepsilon(K)$ will also decrease and approach zero.

II. B.Modeling of single-unit infinite excitation control system

The relationship between current and voltage in the excitation winding between V_f, I_f, r_f, and φ_{fd} can be represented in Figure 2.

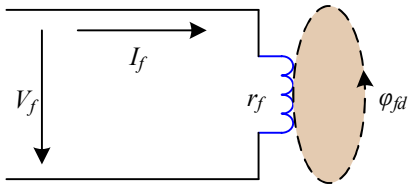

Figure 2: Diagram of the positive direction of the excitation winding

The excitation winding voltage equation can be written as equation (17) from Fig. 2:

$$V_f = r_f I_f + \frac{d\varphi_{fd}}{dt} \tag{17}$$

Eq, V_f - excitation winding voltage, I_f - excitation current, φ_{fd} - total magnetic chain of the excitation winding, r_f - excitation winding resistance.

Multiply x_{ad} / r_f by the terms in the equation, and the collation leads to equation (18):

$$V_f \frac{x_{ad}}{r_f} = x_{ad} I_f + \frac{x_f}{r_f} \frac{d\left(\frac{x_{ad}}{x_f}\right)\varphi_{fd}}{dt} \tag{18}$$

Let $T_{d0} = \frac{x_f}{r_f}$, denote the excitation winding time constant, where x_f is the excitation winding reactance and r_f is its resistance. From equation (19):

$$E_q' = d\left(\frac{x_{ad}}{x_f}\right) \tag{19}$$

The $\varphi_{fd} x_{ad} / x_f$ in Eq. (18) is the transient potential $E_{q'}$ after the d-axis transient reactance $x_{d'}$. And the generator no-load electric potential is shown in equation (20):

$$E_q = x_{ad} I_f \tag{20}$$

At the same time, by making $E_f = V_f \frac{x_{ad}}{r_f}$, Eq. (18) can be written as Eq. (21):

$$E_f = E_q + T_{d0} \frac{dE_q'}{dt} \tag{21}$$

Since $E_f = V_f \frac{x_{ad}}{r_f}$, $\frac{x_{ad}}{r_f}$ is the steady state current I_{ef} of the excitation winding. Since x_{ad} is the mutual inductance between the excitation winding and the d-axis stator winding, the physical significance of $E_f - I_f x_{ad}$ in Eq. (21) is the electromotive force generated by the steady state magnetic chain when the steady state excitation current formed by the rotation of the rotor passes through the d-axis stator winding. Generally, in the process of generator's electric-generated magnetic or magnetic-generated electric, there is a process in the generator excitation winding to ensure that there can be successfully transformed, and this process can be expressed by Equation (21). With the excitation control, the mathematical model of a single-machine infinity power system can be discussed, and its physically simple structure is shown in Fig. 3.

By establishing a mathematical model of the power system that can be practically applied, assuming a transient state, where the mechanical power of the synchronous generator is kept constant during operation, and, at the same time, by considering the excitation time constant as 0, the effect of the transient convex pole effect on the system can be disregarded. Let $\omega_0 = 2\pi f_0$, bring into the formula and organize the simplification can be obtained as equation (22):

$$\dot{\omega} = \frac{\omega_0}{H}\left(P_m - P_e\right) - \frac{D}{H}\omega \tag{22}$$

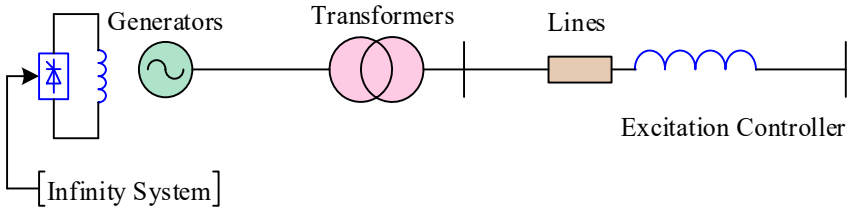

Figure 3: Structure of single infinity bus excitation control system

Bringing the formula into Eq. (21), then Eq. (21) simplifies to Eq. (23):

$$\dot{E}'_q = -\frac{E'_q}{T_{d0}} + \frac{(x_d - x'_d)V_s \cos\delta}{T_{d0}x'_{ds}} + \frac{E_f}{T_{d0}} \tag{23}$$

In this paper, a mathematical model of a third-order single-machine infinity system is developed, which uses the potential of the excitation winding as its control variable as in equation (24):

$$\begin{cases} \dot{\delta} = \omega \\ \dot{\omega} = \dfrac{\omega_0}{H}\left(P_m - P_e\right) - \dfrac{D}{H}\omega \\ \dot{E}'_q = -\dfrac{E'_q}{T_{d0}} + \dfrac{\left(x_d - x'_d\right)V_s \cos\delta}{T_{d0}x'_{ds}} + \dfrac{E_f}{T_{d0}} \\ P_e = \dfrac{E'_q V_s}{x'_{ds}}\sin\delta \end{cases} \tag{24}$$

The final goal of this paper is: the single machine infinity power system studied in this paper can be in the unstable state of its own instability and external input disturbances, the excitation controller needed in this paper is studied, combined with the research method of dynamic output feedback, the generator voltage output is regulated, so that the single machine infinity power system studied in this paper can maintain a stable operation.

II. C. Controller parameter optimization method based on mothballing algorithm

II. C. 1) Fundamentals of the mothballing algorithm

Moth-flame optimization (MFO) algorithms have performance characteristics such as strong parallel optimization capability, good global performance, and not easy to fall into local extremes, and they have been widely used in various fields.

In the MFO algorithm, moths are candidate solutions to the problem to be solved, and the position of moths is a substitution variable. The population matrix M_{nd} of moths is shown in equation (25):

$$M_{nd} = \begin{bmatrix} m_{1,1} & m_{1,2} & \cdots & \cdots & m_{1,d} \\ m_{2,1} & m_{2,2} & \cdots & \cdots & m_{2,d} \\ \vdots & \vdots & \vdots & \vdots & \vdots \\ m_{n,1} & \cdots & \cdots & \cdots & m_{n,d} \end{bmatrix} \tag{25}$$

where n denotes the number of moths and d denotes the dimension of the optimized variable.

The determinant of the fitness of moths O_m is expressed as in equation (26):

$$O_m = \begin{bmatrix} o_{m1} \\ o_{m2} \\ \vdots \\ o_{mn} \end{bmatrix} \tag{26}$$

The flame matrix F_{nd} is defined as in equation (27):

$$F_{nd}=\begin{bmatrix} F_{1,1} & F_{1,2} & \cdots & \cdots & F_{1,d} \\ F_{2,1} & F_{2,2} & \cdots & \cdots & F_{2,d} \\ \vdots & \vdots & \vdots & \vdots & \vdots \\ F_{n,1} & \cdots & \cdots & \cdots & F_{n,d} \end{bmatrix} \tag{27}$$

The fitness value of the flame matrix is expressed in equation (28):

$$O_F=\begin{bmatrix} o_{F1} \\ o_{F2} \\ \vdots \\ o_{Fn} \end{bmatrix} \tag{28}$$

The moth matrix has the same dimension as the flame matrix. In addition, the determinant of the fitness of the moth has the same dimension as the determinant of the fitness of the flame.

The optimization process of moth to flame can be expressed as the optimal solution of the triad as in Eq. (29):

$$MFO=(I,P,T) \tag{29}$$

where the function I that generates the initial position of the moth is as in equation (30):

$$M(i,j)=rand()*(ub(i)-lb(j))+lb(j) \tag{30}$$

where $rand()$ is a function that generates a random number in $(0,1)$. In addition, ub is the maximum value of the variable, as in equation (31):

$$ub=\begin{bmatrix} ub_1 & ub_2 & ub_3 & \cdots & ub_n \end{bmatrix} \tag{31}$$

where lb is the minimum value of the variable and can be defined as in equation (32):

$$lb=\begin{bmatrix} lb_1 & lb_2 & lb_3 & \cdots & lb_n \end{bmatrix} \tag{32}$$

Where P is a function that updates the position of the moth in space and the T function is used to determine if the end condition is satisfied. It is $true$ if the end condition is satisfied and $false$ if the end condition is not satisfied.

The mechanism for updating the position of each moth during the moth search is represented in equation (33):

$$S(M_i,F_j)=D_i\cdot e^{bt}\cdot\cos(2\pi t)+F_j \tag{33}$$

where D_i denotes the displacement from the j th flame to the i th moth, b is a constant that defines the shape of the logarithmic spiral, and t is a random number belonging to the range between $[-1,1]$. The formula for D_i is given in equation (34):

$$D_i=\left|F_j-M_i\right| \tag{34}$$

The MFO algorithm also proposes a mechanism to adaptively adjust the number of flames during each iteration. The formula is shown in equation (35):

$$flame\_no=round\left(N-l*\frac{N-1}{T}\right) \tag{35}$$

where $round()$ is a function that rounds the elements in parentheses to the nearest integer, N denotes the total number of flames, l denotes the current number of iterations, and T denotes the total number of iterations.

The flow of the MFO algorithm is shown in Fig. 4.

II. C. 2) Objective function

In this paper, the PID controller is chosen as the power system stabilizer to suppress the low frequency oscillations.The parameter optimization problem of the PID controller is to determine a set of suitable parameters consisting of K_p, K_i, and K_d to make the system response index optimal.The transfer function of the PID controller, G, is expressed as in Equation (36):

$$G=K_p+\frac{K_i}{s}+K_d\cdot s \tag{36}$$

Common performance metrics include absolute error (IAE), time integral times squared error (ITSE), and time-weighted integral of absolute error (ITAE). The ITAE metric chosen in this paper is defined in equation (37):

$$J=\int_0^{ts} t\times\left|\Delta\omega\right|dt \tag{37}$$

where ts denotes the total simulation time and J is the objective function. Based on this objective function, the optimization problem can be expressed as:

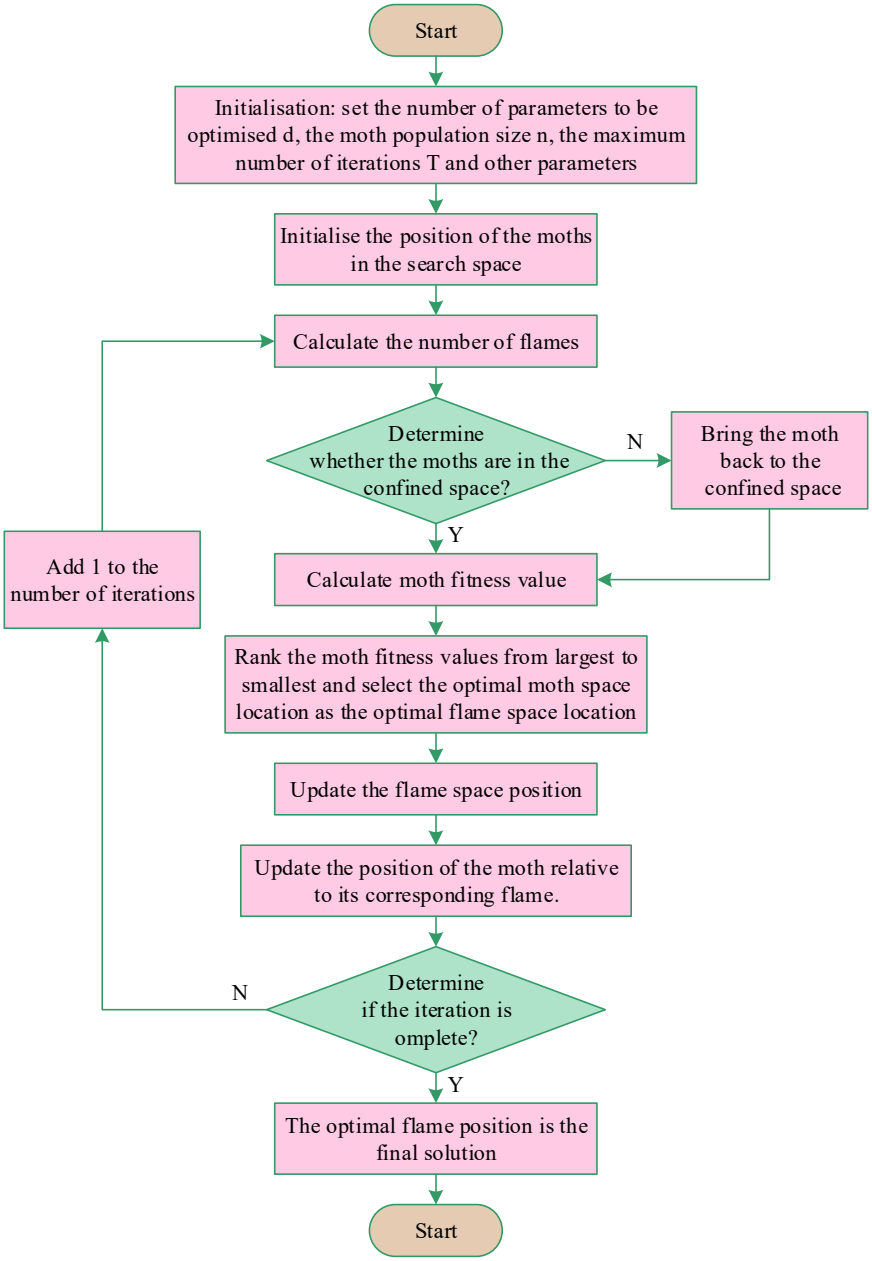

Figure 4: The process of the MFO algorithm

Minimize the objective function J with the constraints of Eq. (38):

$$Subject\ to \begin{cases} K_{p\min} < K_p < K_{p\max} \\ K_{i\min} < K_i < K_{i\max} \\ K_{d\min} < K_d < K_{d\max} \end{cases} \tag{38}$$

where $K_{p\min}$, $K_{p\max}$, $K_{i\min}$, $K_{i\max}$, $K_{d\min}$, $K_{d\max}$ are the upper and lower bounds of the variables to be found K_p, K_i, and K_d are upper and lower bounds.

III. Application Evaluation of Remote Control Strategies

This chapter examines the effectiveness of the power system remote control strategy based on adaptive control algorithm in the form of simulation experiments of the power system under the control strategy, comparison with the simulation numerical results of similar algorithms. It also further explores the role of controller parameters on the performance under the proposed control strategy to provide an effective reference for the control strategy in practical applications.

III. A. Application simulation experiment

Selected with SVC stand-alone power system as the experimental object, the control algorithm in this paper in the far wide (MT) StarSim power electronics real-time experimental platform to complete the simulation experimental verification, the principle structure of the experimental platform mainly includes real-time simulator (NIPXIe-8840), fast controller (NIPXIe-8821), the signal connector (terminal blackTB -60) and the host computer and monitoring software. The tracking error results for the power angle δ are shown in Fig. 5.

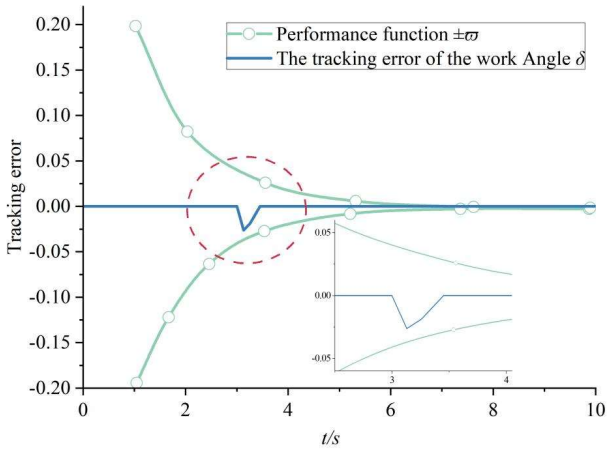

Figure 5: The tracking error of the work Angle δ

The response curve for the power angle δ is shown in Fig. 6.

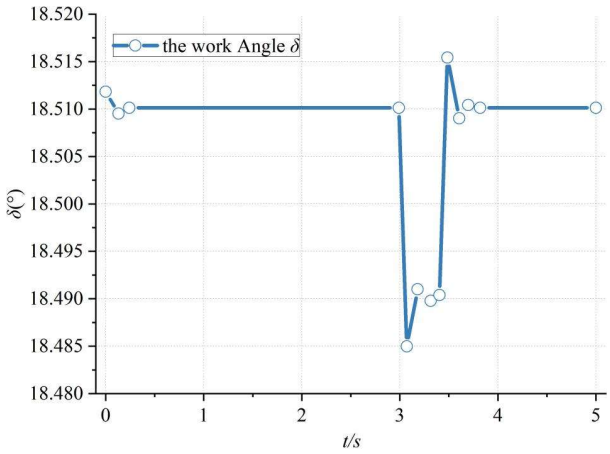

Figure 6: The response curv of the work Angle δ

The results of the response curve for the angular velocity ω are shown in Fig. 7.

It can be seen that after the short-circuit fault disappears, the tracking error curve under the control strategy of this paper can be quickly restored to the stable operation point, thus realizing the expected tracking performance of the power angle. And the system can still maintain a smooth power angle and angular velocity response after a large disturbance.

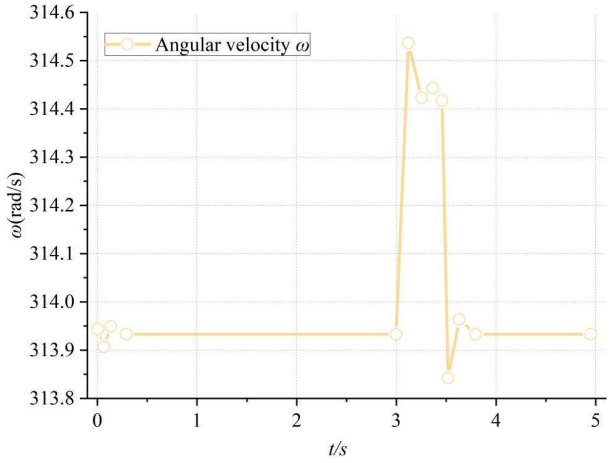

Figure 7: The response curve of angular velocity ω

III. B. Numerical simulation and analysis

In order to check the effectiveness of the method, Matlab/Simulink software is used to numerically simulate the parameter adaptive updating law of the (M1) designed strategy with the (M2) TCSC nonlinear robust controller.

Firstly, we examine whether the operation state of the system is stable when the power system does not add the robust controller μc, i.e., when μc=0. The two-dimensional time series of the observed systems δ and ω are shown in Figs. 8(a) and 8(b), respectively, and at this time, the oscillations of δ and ω present a kind of stochastic oscillation phenomenon that is non-periodic, irregular, and with a tendency of convergence, and therefore it is judged that at this time the systems δ and ω are in the state of chaotic oscillations, and it is clear that at this time the system is no longer stable and reliable, and this kind of oscillations is a good way for the system to be stable, and the system is not a reliable one. Obviously, the system is no longer stable and reliable, and this kind of oscillation is harmful to the system, so it must be controlled.

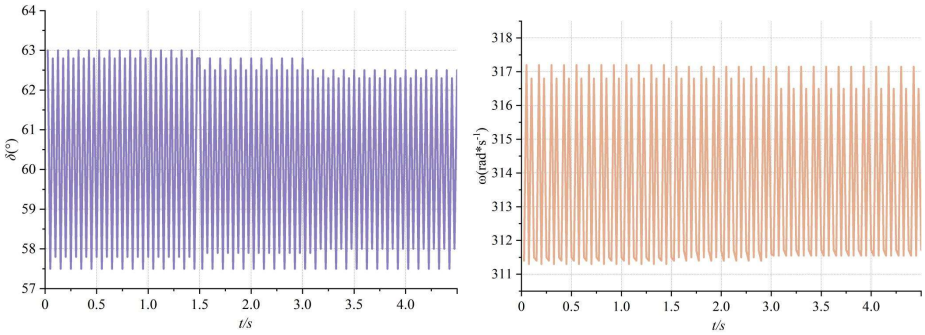

(a) Power Angle of the generator rotor (b) Rotor angular velocity

Figure 8: Two-dimensional timing sequence

A comparison of the results of the two methods in terms of the overall system conductance response curve is shown in Fig. 9. It can be seen that the system reaches the equilibrium operation state in a shorter time (1s) and with smaller oscillation amplitude under the controller modulated by the strategy designed in (M1). Therefore, it shows that the robustness of the controller designed in (M1) is stronger.

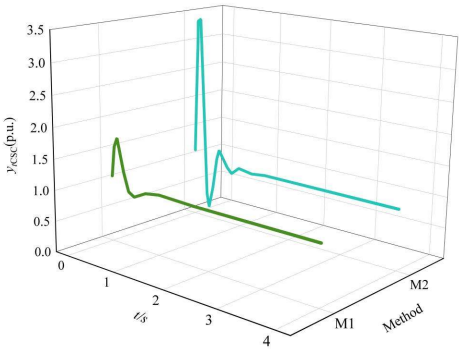

Figure 9: Comparison of the admittance response curves of the overall system

III. C. Analysis of the effect of controller parameters on controller performance

Combined with the actual situation of LFC during power system operation, three cases are designed for simulation experiments. In order to analyze the influence of the controller parameters on the effectiveness of the controller under the control strategy of this paper, this simulation experiment is mainly designed for the main parameters of the controller, frequency deviation c_1, generator active power variation c_2 and generator valve position variation c_3 to compare the three cases.

Case 1: c_1=10, c_2=800, c_3=1000.

Case 2: c_1=0.1, c_2=4000, c_3=1000.

Scenario 3: c_1=0.1, c_2=800, c_3=2000.

The simulation results of each state variable in the system are shown in Fig. 10, which shows that the newly designed controllers with three groups of different parameters all achieve better stable control of the improved system model and effectively limit each state variable to the pre-set range. It is worth noting that the larger the value of c_1, the slower the convergence speed becomes, and the larger the amount of overshooting of state variables x_3 and x_2, but the smaller the overshooting of state variable x_1. And the smaller the value of c_2, the larger the amount of overshooting of all the state variables, the slower the convergence speed, and thus the worse the control effect. c_3 changes have no more obvious effect.

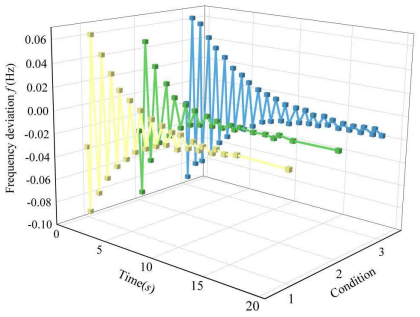

(a) The response of the state variable x1 (frequency deviation)

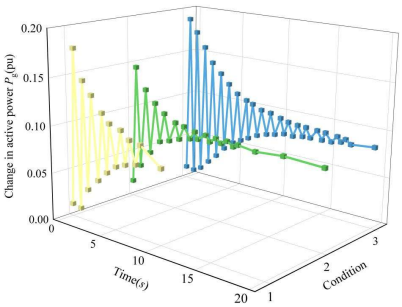

(b) The response of the state variable x2(the change in active power)

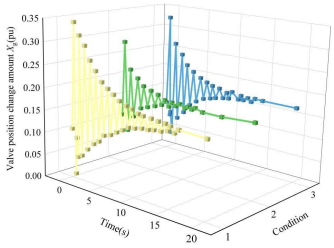

(c) The response of the state variable x3(valve position change amount)

Figure 10: Simulation results of different controller parameters

IV. Conclusion

In this paper, the problem of parameter uncertainty and external perturbation in remote control of power system is materialized into a nonlinear adaptive control problem, and the control algorithm of discrete adaptive neural network is used to estimate the unknown parameters and uncertainty factors. At the same time, the single-machine infinite power system is transformed into a mathematical form, and the mothballing algorithm is used to design the controller and optimize the parameter settings under different time delays, so as to suppress the low-frequency oscillations of the power system. A power system remote control strategy based on adaptive control algorithm is proposed.

The tracking error of the power angle δ of the proposed strategy can be quickly recovered to the stable operation point in the application simulation experiments. In the numerical simulation experiments, the power system to reaches the equilibrium operation state in about 1s, and the overall oscillation amplitude is small. This shows that the power system can maintain a smooth operation state and has excellent performance under the coordination of the adaptive control algorithm. It is worth noting that under the control strategy based on the adaptive control algorithm, the parameter frequency deviation and the variation of generator active power have an important influence on the control effect.

Funding

This research was Supported by Science and Technology Project of Guangxi Power Grid Co., Ltd.: Research on Key Technology of Panoramic Smart Insurance Power Supply System Based on Multi-Modal Artificial Intelligence Big Model and Decision Intelligence Technology (040100KC23110006).

References

[1] Mgenge, M., Swanepoel, J. A., Muvunzi, R., & Daniyan, I. A. (2024). Evaluation of electrical substation automation operational parameters: A systematic literature review. Edelweiss Applied Science and Technology, 8(6), 6360-6373.

[2] Biagini, V., Subasic, M., Oudalov, A., & Kreusel, J. (2020). The autonomous grid: Automation, intelligence and the future of power systems. Energy Research & Social Science, 65, 101460.

[3] Sajadi, A., Strezoski, L., Strezoski, V., Prica, M., & Loparo, K. A. (2019). Integration of renewable energy systems and challenges for dynamics, control, and automation of electrical power systems. Wiley Interdisciplinary Reviews: Energy and Environment, 8(1), e321.

[4] Kabbara, N., Nait Belaid, M. O., Gibescu, M., Camargo, L. R., Cantenot, J., Coste, T., ... & Morais, H. (2022). Towards software-defined protection, automation, and control in power systems: Concepts, state of the art, and future challenges. Energies, 15(24), 9362.

[5] Prostejovsky, A. M., Brosinsky, C., Heussen, K., Westermann, D., Kreusel, J., & Marinelli, M. (2019). The future role of human operators in highly automated electric power systems. Electric Power Systems Research, 175, 105883.

[6] Heidari, S., Fotuhi-Firuzabad, M., & Lehtonen, M. (2017). Planning to equip the power distribution networks with automation system. IEEE Transactions on Power Systems, 32(5), 3451-3460.

[7] Wójtowicz, R., Kowalik, R., & Rasolomampionona, D. D. (2017). Next generation of power system protection automation—virtualization of protection systems. IEEE Transactions on power Delivery, 33(4), 2002-2010.

[8] Alhamrouni, I., Abdul Kahar, N. H., Salem, M., Swadi, M., Zahroui, Y., Kadhim, D. J., ... & Alhuyi Nazari, M. (2024). A comprehensive review on the role of artificial intelligence in power system stability, control, and protection: Insights and future directions. Applied Sciences, 14(14), 6214.

[9] Călin, A. M., Cotfas, D. T., & Cotfas, P. A. (2024). A Review of Smart Photovoltaic Systems Which Are Using Remote-Control, AI, and Cybersecurity Approaches. Applied Sciences, 14(17), 7838.

[10] Nirmal, D. (2020). Artificial intelligence based distribution system management and control. Journal of Electronics, 2(02), 137-47.

[11] Hamdaoui, Y., & Maach, A. (2017, April). An intelligent islanding selection algorithm for optimizing the distribution network based on emergency classification. In 2017 International Conference on Wireless Technologies, Embedded and Intelligent Systems (WITS) (pp. 1-7). IEEE.

[12] Yan, Y., Liu, Y., Fang, J., Lu, Y., & Jiang, X. (2021). Application status and development trends for intelligent perception of distribution network. High Voltage, 6(6), 938-954.

[13] Mahmud, N., & Zahedi, A. (2016). Review of control strategies for voltage regulation of the smart distribution network with high penetration of renewable distributed generation. Renewable and Sustainable Energy Reviews, 64, 582-595.

[14] Antoniadou-Plytaria, K. E., Kouveliotis-Lysikatos, I. N., Georgilakis, P. S., & Hatziargyriou, N. D. (2017). Distributed and decentralized voltage control of smart distribution networks: Models, methods, and future research. IEEE Transactions on smart grid, 8(6), 2999-3008.

[15] Tafti, H. D., Sangwongwanich, A., Yang, Y., Pou, J., Konstantinou, G., & Blaabjerg, F. (2018). An adaptive control scheme for flexible power point tracking in photovoltaic systems. IEEE Transactions on Power Electronics, 34(6), 5451-5463.